Nonlinear Rheology and Structural Changes of $(BS)_n$ Multiblock Copolymers under Shear Flow

Yumi Matsumiya,† Manabu Matsumoto,† Hiroshi Watanabe,*,† Toshiji Kanaya,† and Yoshiaki Takahashi‡

Institute for Chemical Research, Kyoto University, Uji, Kyoto 611-0011, Japan, and Department of Advanced Device Materials, Institute for Material Chemistry and Engineering, Kyushu University, Kasuga, Fukuoka 816-8581, Japan

Received February 5, 2007; Revised Manuscript Received March 17, 2007

ABSTRACT: For a series of 1,4-butadiene (B)−styrene (S) symmetrical multiblock copolymers, BSB triblock, BSBSB pentablock, and BSBSBSB heptablock copolymers having the same block molecular weights and B/S composition, the rheological behavior and structure were examined in dibutyl phthalate (DBP) at 25 °C. DBP is an S-selective solvent, i.e., a good solvent for the S blocks and a poor solvent for the B blocks. The copolymer concentrations C (= 22−25 wt %) were chosen to be just above (by 1 wt %) respective microphase separation concentrations. In a well-equilibrated state, the copolymer/DBP solutions formed a bcc lattice of the spherical domains of unsolved B blocks bridged by the S blocks (lattice-type network), thereby exhibiting elastic behavior under small strains. This lattice-type network was disrupted under steady shear to lose its elasticity, and the heaviest disruption occurred at an intermediate shear rate close to the B/S concentration fluctuation frequency. The elasticity was recovered after cessation of the preshear, and the time t_r^∞ required for full recovery was insensitive to the preshear rate $\dot{\gamma}_{pre}$, i.e., to the magnitude of the network disruption. This behavior suggested that the bridge-type S blocks crossing the flow planes were converted to loops under the preshear, and the re-formation of the bridges, requiring the B blocks to be thermally pulled out from their domain, was the rate-determining step for the recovery. In other words, t_r^∞ of the multiblock copolymers appeared to be primarily determined by the $\dot{\gamma}_{pre}$-insensitive thermodynamic barrier for transient mixing of the pulled out B block into the S/DBP matrix. For such multiblock copolymers, t_r^∞ was found to increase strongly with increasing copolymer molecular weight, and a ratio of t_r^∞ of the triblock, pentablock, and heptablock copolymers was close to 1:5:25. This ratio was consistent with the Rouse/reptation motion of the multiblock chain retarded by the B/S mixing barrier.

1. Introduction

Rheological properties of block copolymers are strongly affected by the microphase-separated structure (shape and long-range order of microdomains) as well as the conformation of the constituent blocks.[1−24] In particular, the effect of the block conformation offers an interesting subject of research related to a difference between BA diblock copolymer and its head-to-head dimer, BAB-type triblock copolymer. The microdomain structure is indistinguishable for these diblock and triblock copolymers,[22,25] but the A block conformation is different. In the microphase-separated state where the B blocks form spherical domains, the A block of the diblock copolymer always has the tail conformation anchored on the B domain, while the A block of the triblock copolymer takes the loop/bridge conformation having the A block ends anchored on the same/different B domain(s). The bridge fraction in a lamella-forming styrene (S)−isoprene (I)−S triblock copolymer system was dielectrically estimated to be[26] ∼0.4 (which agrees with the theoretical value[27,28]), and this fraction decreases on dilution of the SIS copolymer with an I-selective solvent (a good solvent for I and a poor solvent for S), *n*-tetradecane.[10]

For some cases, the difference of the block conformation gives no significant difference in the rheological behavior of diblock and triblock copolymers. For example, a SI diblock copolymer and its dimer SIS triblock copolymers dissolved in *n*-tetradecane form almost identical bcc lattices of glassy S domains to exhibit nearly the same equilibrium modulus under small strains *if the copolymer concentration is not very large and the I blocks are not entangled among themselves.*[10] For this case, the tail-type I block of SI and the dangling loop-type I block of SIS sustain the equilibrium elasticity because of the osmotic interaction stabilizing the lattice,[10,15−17] and their elasticity is similar, in magnitude, to the elasticity of the nonentangled bridge-type I blocks subjected to this interaction.[10] The coincidence of the equilibrium modulus (of the order of $0.1k_BT$ per block[17] with k_BT being the thermal energy) reflects this thermodynamic similarity among the tail-, loop-, and bridge-type blocks.

However, for most of the cases, the difference of the block conformation leads to significant differences in the rheological behavior. For example, the equilibrium modulus sustained by a bridge-type high-M I block in bulk state is larger than the modulus sustained by a corresponding loop-type I block, as demonstrated from beautiful experiments utilizing a SIS triblock copolymer, a SI−vinylpiridine (P) triblock copolymer forming only bridge-type I blocks, and a ring-type SI diblock copolymer forming only loop-type I blocks.[23,24] This difference between the bridge- and loop-type blocks is attributable to a fact that the bridge-type high-M block forms the trapped entanglements, and each trapped entanglement sustains the equilibrium modulus of the order of k_BT (i.e., many k_BT's per bridge) while each loop-type block sustains the equilibrium modulus of the order of k_BT at best unless it forms permanent knots with the other loops.[10]

Even more striking differences are noted for the nonlinear rheological behavior of SI diblock and SIS triblock systems

* To whom correspondence should be addressed.
† Kyoto University.
‡ Kyushu University.

10.1021/ma070306r CCC: $37.00
Published on Web 04/19/2007

forming spherical S domains. Under large strains, the SI system always exhibits plastic flow because the system contains no bridges connecting the S domains.[15−17] In contrast, the SIS system behaves as an elastic solid to exhibit no steady flow but macroscopic rupture under large strains at low T where the S domains bridged by the I blocks are in the glassy state.[8,9] At high T where the S domains are in the liquid state, the SIS system becomes a plastic fluid phenomenologically similar to the SI system.[9] However, even for this case, the mechanism determining the yield stress σ_y is different, as suggested from an experimental fact that σ_y for SI is smaller in homopolyisoprene (hI) than in *n*-tetradecane while σ_y for SIS is larger in hI:[9] The σ_y for the SI system is determined by the stability of the lattice of the S domains therein and thus smaller in hI, a polymeric I-selective solvent that screens the osmotic interaction stabilizing the lattice. In contrast, σ_y of the SIS system is larger in hI because the S blocks connected to the bridge-type I blocks are transiently pulled out/mixed in the I matrix phase under the flow,[5,6,9] and the barrier for this mixing, which determines σ_y of the SIS system, is larger in hI.

Focusing on such rheological differences between the diblock and triblock copolymer systems, we recently examined the rheology and structure of a butadiene−styrene (BS) diblock[19] and its dimer BSB triblock[22] copolymers in dibutyl phthalate (DBP). DBP is a S-selective[20,21] solvent, i.e., a good solvent for the S blocks and a poor solvent for the B blocks. We found that the bcc lattice of the spherical B domains, commonly formed in the BS and BSB systems at equilibrium to provide the systems with elasticity, is disrupted under shear flow, and a magnitude of disruption is determined by a balance of the flow rate and the frequency of B/S concentration fluctuation.[19,22] Although this disruption behavior was similar for the BS and BSB systems, the elasticity recovery behavior after the shear was quite different. The recovery for BS was the slowest for the most heavily disrupted lattice, as naturally expected.[19] In contrast, the recovery rate for BSB was insensitive to the magnitude of the lattice disruption.[22] This peculiar behavior was related to the flow-induced conversion of the bridge-type S blocks to the loops: The elasticity of BSB is fully recovered only when the bridges are re-formed from the loops, and this re-formation requires the B blocks connected to the loop-type S blocks to be thermally pulled out/mixed into the S/DBP matrix phase. Then, the B/S mixing barrier governs the recovery rate irrespective of the magnitude of the lattice disruption, as observed.

The above results for the BS and BSB systems demonstrate that the dynamics of the copolymer chains is strongly affected by their architecture. It is of interest to examine this effect for multiblock copolymers having more than two inner blocks. Thus, we have synthesized a series of symmetrical BSB triblock, BSBSB pentablock, and BSBSBSB heptablock copolymers and examined the rheological behavior of their solutions in DBP under steady shear flow and after cessation of flow. It turned out that the behavior of the pentablock and heptablock copolymers is qualitatively similar to but quantitatively different from the behavior of the triblock copolymer. In particular, the time t_r^∞ required for full recovery of the equilibrium elasticity after cessation of flow was significantly different: t_r^∞ was longer in the order of triblock < pentablock < heptablock. This paper presents details of these results and discusses the difference of t_r^∞ in relation to the block chain motion affected by the B/S mixing barrier.

Scheme 1. Synthetic Route of the Copolymer Samples

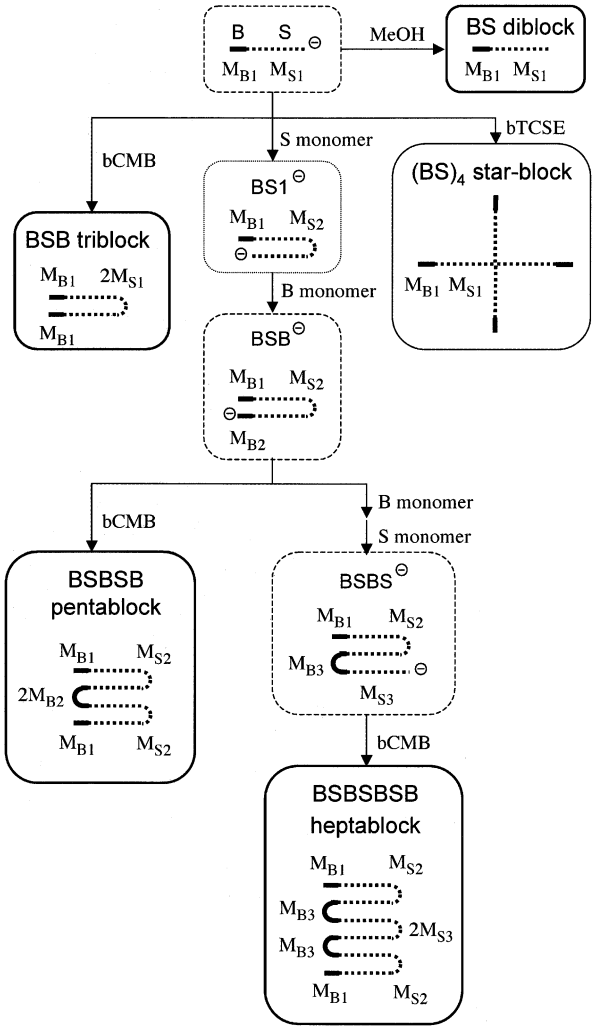

2. Experimental Section

2.1. Materials. A series of symmetrical 1,4-butadiene (B)−styrene (S) multiblock copolymers, BSB triblock, BSBSB pentablock, and BSBSBSB heptablock copolymers, were synthesized via stepwise living anionic polymerization followed by coupling with 1,4-bis(chloromethyl)benzene (bCMB). The synthesis was made with a standard vacuum technique utilizing glass flasks/ampules, constrictions, and breakable seals.[29−31] The B blocks were made with a deuterated monomer so that they had the neutron scattering contrast from the S blocks made with a protonated monomer. The polymerization solvent was benzene, and the initiator was *sec*-butyllithium obtained from a direct reaction of *sec*-butyl chloride and Li metal in heptane. The deuterated B monomer was purchased from CDN isotopes, 1,2-bis(trichlorosilyl)ethane (bTCSE) utilized as a multifunctional coupler was purchased from Tokyo Kasei, and all other chemicals, including tetrahydrofuran (THF) utilized as a solvent for bCMB and bTCSE and methanol utilized as a terminator, were purchased from Wako. These chemicals were purified with standard methods.[29−31]

The route of the stepwise polymerization of the samples is shown in Scheme 1. After each step of polymerization, precursors were recovered for convenience of characterizing the samples. First, BS$^-$ diblock anion chains were synthesized with *sec*-butyllithium in benzene and split into four batches. The BS$^-$ chains in the first batch were terminated with methanol (MeOH) to recover the BS diblock sample. The BS$^-$ chains in the second and third batches were allowed to react with bifunctional and tetrafunctional couplers, respectively, bCMB and bTCSE both being diluted with THF, to give the BSB triblock and (BS)$_4$ 4-arm star-block samples, the latter to be utilized in our future study. (bTCSE works as the tetrafunc-

Table 1. Characteristics of Block Copolymer Samples[a]

	BS diblock	BSB triblock	BSBSB pentablock	BSBSBSB heptablock	$(BS)_4$ star block[i]
$10^{-3}M_B$ of first block (B)	15.5[b]	15.5[b]	15.5[b]	15.5[b]	15.5[b]
$10^{-3}M_S$ of second block (S)	80.6[c]	161.2[d]	160.8[e]	160.8[e]	80.6[c]
$10^{-3}M_B$ of third block (B)		15.5[b]	30.8[f]	31.5[g]	
$10^{-3}M_S$ of fourth block (S)			160.8[e]	156.0[h]	
$10^{-3}M_B$ of fifth block (B)			15.5[b]	31.5[g]	
$10^{-3}M_S$ of sixth block (S)				160.8[e]	
$10^{-3}M_B$ of seventh block (B)				15.5[b]	

[a] M shown in this table stands for weight-average molecular weight. The polydispersity index was smaller than 1.05 for all samples. [b] Identical to M_{B1} shown in Scheme 1. For the star block, the B block in each arm has M_{B1}. [c] Identical to M_{S1} shown in Scheme 1. For the star block, the S block in each arm has M_{S1}. [d] Identical to $2M_{S1}$ shown in Scheme 1. [e] Identical to M_{S2} shown in Scheme 1. [f] Identical to $2M_{B2}$ shown in Scheme 1. [g] Identical to M_{B3} shown in Scheme 1. [h] Identical to $2M_{S3}$ shown in Scheme 1. [i] To be utilized in the future work.

tional coupler for the polystyrenyl anion because of the large steric hindrance of this anion.[32,33]) The mole numbers of these couplers were set to be ~90% equimolar to the anions in order to ensure the high efficiency of the coupling reactions. The crude products of these coupling reactions were repeatedly fractionated from benzene/methanol mixtures to recover the purified triblock and star-block samples.

The BS^- anion chains in the fourth batch were allowed to react with the S monomer to give $BS1^-$ and then with the B monomers to give BSB^- (cf. Scheme 1). The BSB^- chains (in the benzene solution) were split into two batches, and the chains in one batch were coupled with bCMB (~90% equimolar to the anions) to give the BSBSB pentablock copolymer. The BSB^- chains in the other batch were allowed to sequentially react with prescribed volumes of B and S monomers to give $BSBS^-$ anion chains, and these anion chains were coupled with bCMB (~90% equimolar to the anions) to give the BSBSBSB heptablock copolymer. The crude products of these coupling reactions were fractionated from benzene/methanol mixtures to recover the purified pentablock and heptablock samples.

The block copolymer samples thus obtained and the precursors recovered after each step of polymerization were characterized with GPC (Co-8020 and DP8020, Tosoh) equipped with a refractive index (RI)/low-angle light scattering (LALS) monitor (LS-8000, Tosoh) and an ultraviolet (UV) adsorption monitor (UV-8020, Tosoh) connected in series. THF was the eluent, and previously synthesized/characterized monodisperse polybutadienes[34] and commercially available monodisperse polystyrenes (TSK's, Tosoh) were utilized as the elution standards as well as the reference materials for the RI/LS/UV signal intensities. The characterization was made with the standard method explained in Appendix A, and the results are summarized in Table 1.

Since our BSB triblock, BSBSB pentablock, and BSBSBSB heptablock samples were synthesized through the head-to-head coupling of respective precursor anions, they had the symmetric architecture. It should be noted that all samples were synthesized from the same batch of BS^- precursor and had the same M_B for the end B block (cf. Table 1). Furthermore, the molecular weights of the inner blocks were very similar for the triblock, pentablock, and heptablock samples because the volumes of the S and B monomers utilized in respective steps of polymerization and the volumes of the precursor solutions taken from the polymerizing batches were carefully measured with long ampules having fine grids.

The materials subjected to rheological and neutron scattering measurements were solutions of the triblock, pentablock, and heptablock samples in dibutyl phthalate (DBP), a good solvent for the S blocks and a poor solvent for the B blocks. For comparison, a DBP solution of the diblock sample was also examined. These solutions were prepared by uniformly dissolving prescribed masses of the copolymer samples and DBP in excess of a cosolvent, benzene, and then allowing benzene to completely evaporate.

At 25 °C, the solutions exhibited a sharp transition from fluid to plastic solid on a small increase of concentration (by 1 wt %), as similar to the behavior of the previously examined BS and BSB samples.[19,22] This transition reflected the formation of the lattices of the B domains bridged by the S blocks in the triblock, pentablock, and heptablock solutions and the formation of the lattice without the bridges in the diblock solution. Thus, the concentrations C of the copolymers were chosen to be 1 wt % higher than respective transition concentrations: $C = 24.0$, 25.0, 22.0, and 22.5 wt % for the diblock, triblock, pentablock, and heptablock samples, respectively. (These C values were chosen because the elasticity recovery after cessation of preshear was intractably slow for the pentablock and heptablock solutions at higher C.)

2.2. Measurements. For the DBP solutions of the diblock, triblock, pentablock, and heptablock copolymers prepared as above, rheological measurements were carried out at 25 °C with a laboratory rheometer (ARES, Rheometrics). A cone−plate fixture with the plate diameter = 25.0 mm and the gap angle = 0.1 rad was used. In the dynamic measurements, the amplitude of the oscillatory strain was kept small ($\gamma_0 = 0.01$) to ensure the linearity of the storage and loss moduli, $G'(\omega)$ and $G''(\omega)$, measured as functions of the angular frequency ω.

The copolymer solutions were charged in the rheometer at 70 °C, kept at 70 °C for 15 min, quiescently cooled to 25 °C, and then annealed at 25 °C for 36 h. After this annealing process, all solutions exhibited the elastic behavior under small strains at low ω. This elasticity resulted from a lattice-type network of the B domains connected by the S bridges (for the cases of the triblock, pentablock, and heptablock copolymers) and the lattice of the B domains without the bridges (for the case of diblock copolymer), as revealed from small-angle neutron scattering (SANS). The long annealing time of 36 h was required to well equilibrate this structure and stabilize the elastic response, in particular for the pentablock and heptablock solutions.

For the copolymer/DBP solutions equilibrated at 25 °C, the steady-state viscosity $\eta(\dot{\gamma})$ was measured at various shear rates $\dot{\gamma}$. For all solutions, the lattice of the B domains was disrupted to various magnitudes according to the $\dot{\gamma}$ value, as confirmed from SANS measurements under flow. Correspondingly, the G' at low ω measured immediately after cessation of the steady shear was smaller than the equilibrium modulus. During the quiescent rest after the shear, linear viscoelastic measurements were made to trace a change (increase) of G' with the time. This change reflected a recovery of the lattice of the B domains.

For the copolymer solutions, the SANS measurements were made with the SANS-U spectrometer at the Neutron Scattering Laboratory, Institute for Solid State Physics, University of Tokyo (Tokai, Ibaragi). The incident neutron wavelength was $\lambda = 0.7$ nm with a wavelength spread of $\Delta\lambda/\lambda = 0.1$, the beam diameter was 0.3 cm, and the sample-to-detector distance was set at 4.0 m. The scattering intensity was measured as a function of the scattering vector $\mathbf{q}$, where $q = |\mathbf{q}| = [4\pi/\lambda] \sin(\theta/2)$ with θ being the scattering angle. The measurements were made at 25 °C in a Couette flow cell[35] with the inner and outer radii of 25.25 and 27.00 mm, respectively. The system was quiescently ordered in the cell (by cooling from 70 to 25 °C), and the SANS profiles were obtained at equilibrium and under steady shear. The incident beam was in the direction of the velocity gradient, and the profiles were detected in a velocity−vorticity plane. The SANS profiles were azimuthally symmetric within experimental resolutions (except for the diblock and triblock solutions sheared at $\dot{\gamma}/s^{-1} = 0.1$ and 0.01, respectively), indicating that the lattice of the B domains was not significantly shear-oriented

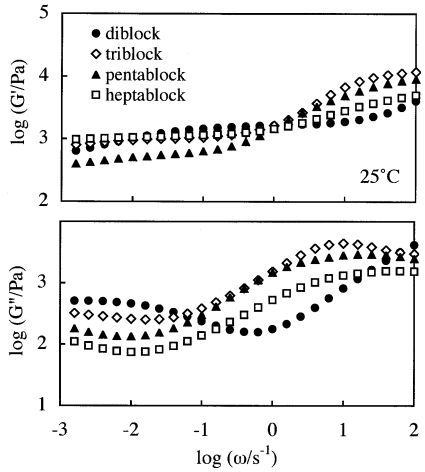

Figure 1. Linear viscoelastic moduli measured for DBP solutions of diblock, triblock, pentablock, and heptablock copolymers with C = 24.0, 25.0, 22.0, and 22.5 wt % well equilibrated at 25 °C.

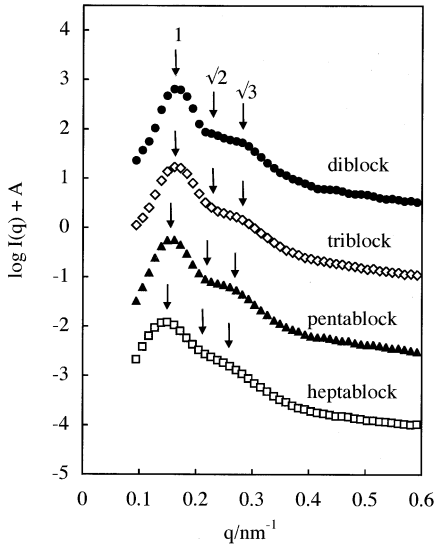

Figure 2. SANS profiles of DBP solutions of diblock, triblock, pentablock, and heptablock copolymers with C = 24.0, 25.0, 22.0, and 22.5 wt % well equilibrated at 25 °C. The profiles for the triblock, pentablock, and heptablock copolymers are shifted vertically by factors of $A = -1.5$, -3, and -4.5 in order to avoid heavy overlapping of the profiles.

in most cases. In this paper, we present the circularly averaged profiles $I(q)$ without a correction for the incoherent scattering. These profiles were sufficient for the discussion in this paper.

3. Results and Discussion

3.1. Linear Viscoelastic Behavior and Structure at Equilibrium. For the diblock and multiblock copolymer solutions equilibrated at 25 °C, Figure 1 shows the ω dependence of the storage and loss moduli, G' and G'', and Figure 2 shows their SANS profiles $I(q)$ obtained with the same exposure time of 20 min. The profiles for the triblock, pentablock, and heptablock copolymers are shifted vertically by factors of $A = -1.5$, -3, and -4.5 in order to avoid heavy overlapping of the plots. (The contrast between the deuterated B and protonated S blocks enabled us to readily examine the microdomain structure with SANS.)

As seen in Figure 2, all solutions exhibit the scattering peak/shoulders at the scattering vectors q of a ratio of $1:\sqrt{2}:\sqrt{3}$ (cf. arrows), which is attributable to the interference between the spherical B domains (minor component not dissolved in DBP).

Table 2. BCC Lattice Parameters for Copolymer/DBP Solutions Equilibrated at 25 °C

	C/wt %	D^a/nm	a^b/nm	$r_B{}^c$/nm
BS diblock	24.0	47.8	55.2	9.6
BSB triblock	25.0	47.8	55.2	9.7
BSBSB pentablock	22.0	50.0	57.7	9.7
BSBSBSB heptablock	22.5	52.0	60.0	10.3

[a] D = nearest-neighbor distance = $2\pi\sqrt{3/2}/q_1$. [b] a = cell edge length = $2D/\sqrt{3}$. [c] $r_B = (3\phi_B a^3/8\pi)^{1/3}$ with ϕ_B being the B block volume fraction in the solution. (This r_B was evaluated under an assumption of no swelling of the B domain with DBP.)

Thus, the copolymer chains form lattices of the B domains, quite possibly bcc lattices as judged from this q ratio. The lattices in the triblock, pentablock, and heptablock solutions appear to be considerably distorted, as judged from the broadness of the higher order shoulders. The lattice parameters evaluated from the q_1 value of the first-order scattering peak are summarized in Table 2. Neighboring B domains in the triblock, pentablock, and heptablock solutions should be connected by the bridge-type S blocks coexisting with the loops, while no bridge exists in the diblock solution. These lattice structures, either with or without the bridges, provide the solutions with the elasticity characterized by the low-ω plateau of G' seen in Figure 1.

Here, a comment needs to be added for the increase of G'' (almost equivalent to an increase of tan $\delta = G''/G'$) seen for all solutions on a decrease of ω from 10^{-2} to 10^{-3} s^{-1}. This increase of G'', associated with a mild decrease of G', indicates that the solutions exhibit an ultraslow relaxation process at $\omega < 10^{-3}$ s^{-1} that is similar to the process seen for a bulk S-hydrogenated B−S triblock copolymer.[36] This ultraslow process may be related to the fluctuation of the lattice structure as well as the thermal migration of individual B blocks from one domain to the others. Simultaneous/cooperative migration of many B blocks, a process required for full relaxation of the lattice, should be tremendously slower than the uncorrelated migration of individual B blocks. Thus, *in a practical sense*, the equilibrated diblock and multiblock solutions exhibit a static elasticity in our experimental window. For simplicity, this elasticity is hereafter referred to as equilibrium elasticity, and G' at the lowest ω examined (= 1.6×10^{-3} s^{-1}) is regarded to be the equilibrium modulus, G_e.

The G_e value is similar in magnitude for the diblock and multiblock solutions all having nearly the same C, in particular for the diblock, triblock, and heptablock solutions (cf. Figure 1). For these solutions, the entanglement molecular weight for the S block in the S/DBP matrix phase is estimated to be $M_e = M_e{}^o/\phi_S{}^{1.3} \cong 130 \times 10^3$, with $M_e{}^o$ (= 18×10^3)[37] and ϕ_S being the M_e value for bulk polystyrene and volume fraction of the S blocks in the matrix phase, respectively. The molecular weight of the S blocks of the multiblock copolymer samples, $M_S \cong 160 \times 10^3$ (cf. Table 1), is just comparable with this M_e. Thus, individual S blocks would have been entangled only lightly in the matrix phase. The tail-type S block of the diblock copolymer and the lightly entangled loop/bridge-type S block of the multiblock copolymers should exhibit the equilibrium moduli of similar magnitudes in the presence of the osmotic interaction,[10] as observed in Figure 1. In relation to this point, we should emphasize that the G_e value (= 500−1000 Pa) reduced to each S block is of the order of $0.1k_BT$, not of the order of k_BT expected for the simplest rubber elasticity, because of the osmotic correlation[17] of the conformations of neighboring S blocks.

The triblock, pentablock, and heptablock solutions exhibit a fast relaxation process characterized by the G'' peak at high ω

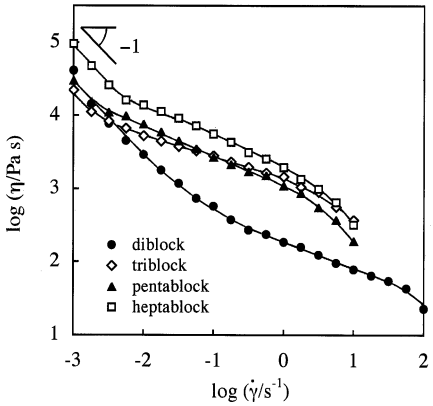

Figure 3. Steady-state viscosity of DBP solutions of diblock, triblock, pentablock, and heptablock copolymers with $C = 24.0$, 25.0, 22.0, and 22.5 wt % at 25 °C.

(cf. Figure 1). This peak, commonly seen at $\omega \cong 10$ s^{-1} for these solutions, is attributable to the motion of individual bridge/loop-type S blocks (having almost identical M_S in the three multiblock samples; cf. Table 1). This assignment is consistent with the relaxation time data for homopolystyrene (hS)/DBP solutions.[38] Similarly, a fast relaxation process of the diblock solution, reflected in the increase of G'' on an increase ω from 1 to 100 s^{-1}, can be attributed to the motion of the tail-type S blocks therein (with $M_S \cong 80 \times 10^3$).

In Figure 1, we also note a difference between the multiblock solutions that the G'' peak at $\omega \cong 10$ s^{-1} broadens and decreases its height with increasing copolymer molecular weight, M_{copol}. This difference may be related to a difference in the efficiency of the trapped entanglement formation: The solutions were prepared via evaporation of the cosolvent, benzene, and the trapped entanglements would have been formed (though lightly) at the point of microphase separation during the evaporation process.[39] This entanglement formation should have been more efficient for the copolymer chains overlapping more heavily at that point, i.e., for larger M_{copol}. The trapped entanglement subdivides the S blocks into smaller network sections to broaden their relaxation, which naturally results in the broadening and height decrease of the G'' peak seen in Figure 1. The difference in the efficiency of the entanglement formation might have also contributed to a moderate difference in the G_e values of the three multiblock solutions.

At the same time, no dense entanglement should have been formed for individual S blocks in the solutions, as judged from the G_e value (of the order of $0.1k_BT$ per each S block) and the close coincidence of the M_e and M_S values. Keeping this point in our mind, we examine the nonlinear flow behavior and the corresponding structure of the copolymers in the following sections.

3.2. Nonlinear Behavior and Lattice Disruption under Shear Flow. Figure 3 shows the shear rate ($\dot\gamma$) dependence of the steady-state viscosity η measured for the diblock and multiblock solutions at 25 °C. The measurement was conducted for the equilibrated solutions in the order of increasing $\dot\gamma$. For all solutions, η is inversely proportional to $\dot\gamma$ (i.e., the plastic behavior prevails) at sufficiently low $\dot\gamma$, but the $\dot\gamma$ dependence becomes weaker at high $\dot\gamma$. We also note that the diblock copolymer exhibits the plastic behavior in a wider range of $\dot\gamma$ (up to 0.1 s^{-1}) compared to the triblock, pentablock, and heptablock copolymers and that the latter three have roughly the same η data (despite a difference of their molecular weight). This result suggests a difference in the flow mechanism: The diblock solution contains no bridge connecting the micellar B cores therein and thus flows without pulling out the B blocks from the cores, while the flow in the multiblock solutions is associated with the pullout of the B blocks connected to the bridge-type S blocks therein. The flow-induced changes in the lattice structure of the B domains, which should correspond to these flow mechanisms, were detected from the rheo-SANS measurements under the steady shear flow.

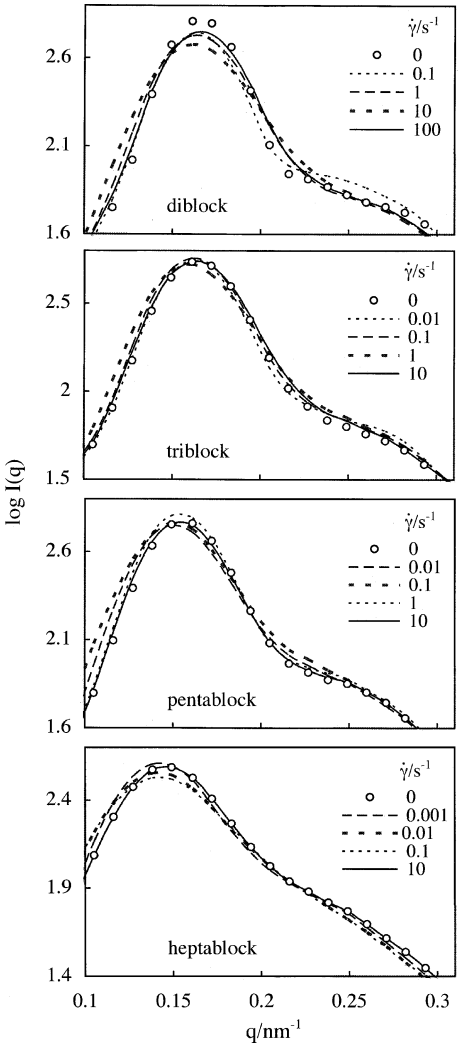

Figure 4. SANS profiles of DBP solutions of diblock, triblock, pentablock, and heptablock copolymers with $C = 24.0$, 25.0, 22.0, and 22.5 wt % measured under steady shear at 25 °C (curves). The circles indicate the profile at equilibrium ($\dot\gamma = 0$).

The SANS intensities $I(q)$ of the solutions measured in the velocity−vorticity plane were azimuthally symmetric, except for the diblock and triblock solutions that exhibited shear orientation of the lattice of the B domains at $\dot\gamma = 0.1$ and 0.01 s^{-1}, respectively. For convenience of our discussion of the flow-induced disruption of the lattice, the profiles were circularly averaged for all cases (including these exceptional cases). Figure 4 presents these profiles magnified around the scattering peaks where this disruption behavior is most clearly observed.

In Figure 4, the circles indicate the SANS profiles of the solutions in the well-equilibrated state. Under the flow, the first-order peak becomes broader and the higher order peaks/shoulder are smeared. These changes in the SANS profile are indicative of the flow-induced disruption of the lattice of the B domains, being associated with the pullout of the B blocks (connected to the S bridges) in the multiblock solutions and without this pullout in the diblock solution. This lattice disruption does not

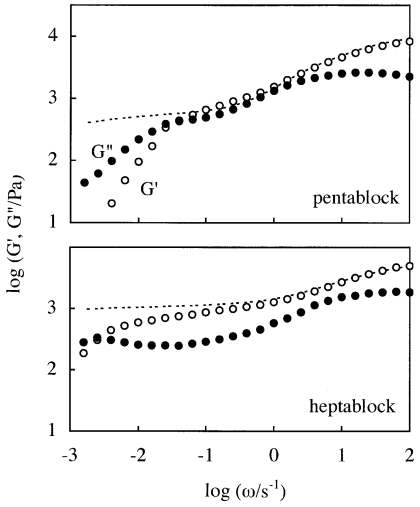

Figure 5. Linear viscoelastic storage and loss moduli (unfilled and filled circles) measured for DBP solutions of pentablock and heptablock copolymers with $C = 22.0$ and 22.5 wt % just after the steady preshear. The dotted curves indicate the storage modulus at equilibrium.

proceed monotonically with increasing $\dot{\gamma}$. Instead, the heaviest disruption (seen as the largest deviation of the SANS profile from that at equilibrium) occurs at intermediate shear rates, $\dot{\gamma}_c/s^{-1} \cong 10$, 1, 0.1, and 0.01 for the diblock, triblock, pentablock, and heptablock solutions, and the flow at $\dot{\gamma} > \dot{\gamma}_c$ gives less significant disruption. In particular, the profiles for the pentablock and heptablock solutions under the shear at $\dot{\gamma} = 10\ s^{-1}$ ($\gg\dot{\gamma}_c$) are very close to the profiles at equilibrium.

This nonmonotonic disruption behavior can be interpreted in relation to the frequency ω_f of B/S concentration fluctuation:[19,22] Namely, this fluctuation should survive under the shear at $\dot{\gamma} < \omega_f$ to assist the spatial transformation of the copolymer chains thereby tending to repair the flow-disrupted lattice, while the fluctuation should be quenched at $\dot{\gamma} > \omega_f$ to allow formation of flat and continuous flow planes that protect the majority of the grains of the lattice from the shear-induced disruption. Thus, the lattice would be most heavily disrupted at $\dot{\gamma} \cong \omega_f$ where none of these mechanisms work efficiently.

The viscoelastic relaxation attributable to the B/S concentration fluctuation was observed for our pentablock and heptablock solutions just after the preshear, as demonstrated in Figure 5. The equilibrium plateau of G' (shown with the dotted curves) vanishes by the preshear, and the terminal relaxation is seen in the absence of this plateau. This relaxation is much slower than the relaxation of individual blocks (occurring at $\omega \geq 10\ s^{-1}$) and attributable to the fluctuation.[19,22] The fluctuation frequencies evaluated as the $G'-G''$ crossing frequency, $\omega_f/s^{-1} \cong 0.03$ and 0.003 for the pentablock and heptablock solutions, are in the vicinity of the critical shear rates for the heaviest lattice disruption in respective solutions, $\dot{\gamma}_c/s^{-1} \cong 0.1$ and 0.01. This result is in harmony with the above molecular interpretation.

For the presheared pentablock and heptablock solutions, the terminal relaxation due to the fluctuation was successfully detected in our measurement because their elasticity recovery time t_r^∞ ($\geq$14 h, as shown later) was longer than the time ($\cong$7 h) necessary for the measurement covering ω/s^{-1} from 100 to 1.6×10^{-3}. For the diblock and triblock solutions, the recovery was significantly faster ($t_r^\infty < 5$ h) and thus occurred during our measurement. For this reason, G' of the diblock and triblock solutions (not shown here) decreased from the equilibrium plateau but did not exhibit the terminal relaxation. However, the shear rates for the heaviest lattice disruption in these solutions, $\dot{\gamma}_c/s^{-1} \cong 10$ and 1 (cf. Figure 4), should correspond to the fluctuation frequencies ω_f in respective solutions, as judged from the close agreement of $\dot{\gamma}_c$ and ω_f found for similar solutions.[19,22]

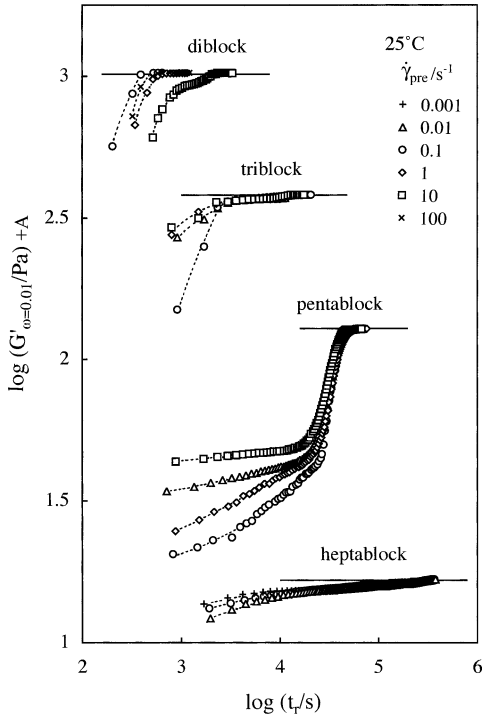

Figure 6. Time-dependent changes of $G'(\omega = 0.01\ s^{-1})$ measured for DBP solutions of diblock, triblock, pentablock, and heptablock copolymers with $C = 24.0$, 25.0, 22.0, and 22.5 wt % after the preshear at the rates as indicated. The horizontal solid lines indicate the G' values in the fully equilibrated state. The data for the triblock, pentablock, and heptablock solutions are vertically shifted by factors of $A = -0.4$, -0.6, and -1.8 to avoid heavy overlapping of the plots.

3.3. Elasticity Recovery after Preshear. For the diblock and multiblock copolymer solutions, we measured the storage modulus G' at $\omega = 0.01\ s^{-1}$ (well in the low-ω plateau zone at equilibrium) as a function of the time t_r after cessation of preshear at various rates $\dot{\gamma}_{pre}$. The amplitude of oscillatory strain was kept small (=0.01) so that the measurement did not disturb the elasticity recovery after the preshear. Figure 6 shows double-logarithmic plots of the G' data against t_r. The data for the triblock, pentablock, and heptablock solutions are vertically shifted by factors of $A = -0.4$, -0.6, and -1.8 to avoid heavy overlapping of the plots. The horizontal solid lines indicate the G' values of respective solutions ($\omega = 0.01\ s^{-1}$) in the well-equilibrated state shown in Figure 1.

As seen in Figure 6, the G' value increases with t_r and approaches the final value (equilibrium value) at sufficiently long t_r. One may suspect that this elasticity recovery is faster for heptablock solution than for the pentablock solution because the transient G' value at $t_r \sim 10^4$ s deviates from the final value less significantly for the former. However, this is not the case: For $\omega = 0.01\ s^{-1}$, the initial value of G' just after the preshear is considerably larger for the heptablock solution because the B/S concentration fluctuation is much slower for this solution than for the pentablock solution (see Figure 5), while the final value of G' is nearly the same for these solutions. Thus, during the elasticity recovery process, a ratio of the final value of G' to the initial value is much smaller for the heptablock solution, thereby giving the small deviation mentioned above. Actually, the time t_r^∞ for the full recovery of the elasticity evaluated from the data in Figure 6 was longer for the heptablock solution.

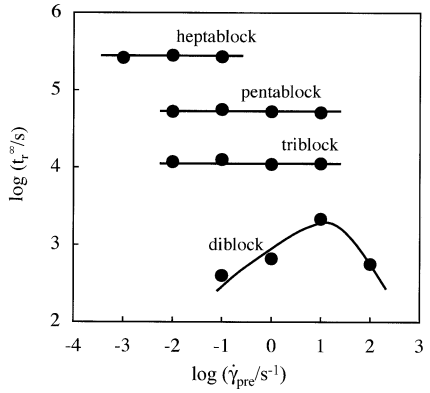

Figure 7. The time t_r^∞ required for full recovery of the equilibrium elasticity of DBP solutions of diblock, triblock, pentablock, and heptablock copolymers with C = 24.0, 25.0, 22.0, and 22.5 wt % presheared at 25 °C. This t_r^∞ is double-logarithmically plotted against the preshear rate.

In Figure 7, the t_r^∞ data for all solutions are plotted against the preshear rate $\dot{\gamma}_{pre}$. For the diblock solution, t_r^∞ clearly changes with $\dot{\gamma}_{pre}$: The t_r^∞ is the longest at $\dot{\gamma}_{pre} = 10\ s^{-1}$ where the lattice of the B domains was most heavily disrupted (cf. top panel of Figure 4). This result strongly suggests that the elasticity recovery in this solution corresponds to the re-formation of the lattice through the motion of the B domains having no bridge-type S blocks,[40] as fully discussed previously.[19]

In contrast, t_r^∞ required for the full recovery of the elasticity in the multiblock solutions hardly changes with $\dot{\gamma}_{pre}$, although the partial recovery rate at short times changes with $\dot{\gamma}_{pre}$ (see Figures 6 and 7). The lattice of the B domains in these solutions is disrupted to different magnitudes according to the $\dot{\gamma}_{pre}$ value (cf. Figure 4). Thus, the $\dot{\gamma}_{pre}$ insensitivity of t_r^∞ suggests that the bridge-type S blocks crossing the flow plane are converted to the loops during the preshear[5,6] and the elasticity recovery requires the re-formation of the bridges (that stitch the flow plane and allow the full re-formation of the lattice).[22] For the conversion of the loop-type S block into the bridge, it has to pull out the connected B block from the B domain and transfer this B block to the other domain through the S/DBP matrix phase. Thus, the re-formation of the bridges is associated with a transient B/S mixing, and the thermodynamic barrier (free energy increment) for this mixing should determine the rate of bridge re-formation to give the $\dot{\gamma}_{pre}$-insensitive t_r^∞.

3.4. Dynamics during Elasticity Recovery for Multiblock Solutions. The triblock, pentablock, and heptablock solutions exhibit the qualitatively similar elasticity recovery behavior characterized by the $\dot{\gamma}_{pre}$-insensitive t_r^∞. However, we also note a quantitative difference: The three horizontal lines in the double-logarithmic plots in Figure 7 have an almost equal spacing of 0.7, and thus the ratio of the t_r^∞ values of those solutions is close to $1:10^{0.7}:10^{1.4} \cong 1:5:25$. This ratio can be related to the dynamics of the multiblock copolymer chains, as discussed below.

The elasticity recovery of the multiblock solutions is attributable to the re-formation of bridges that stitch the flow planes made by the preshear.[22] This re-formation, occurring through the equilibrium motion of the multiblock copolymer chain as a whole, requires the B blocks to be thermally pulled out/mixed in the S/DBP matrix phase. Since the copolymer chain motion after this pullout should be much faster compared to the pullout process itself, the effective friction for the chain motion would be determined by the thermodynamic barrier for the B/S mixing.

Thus, we may model the copolymer chains as illustrated in Figure 8. The B block located at the end of all copolymer chains

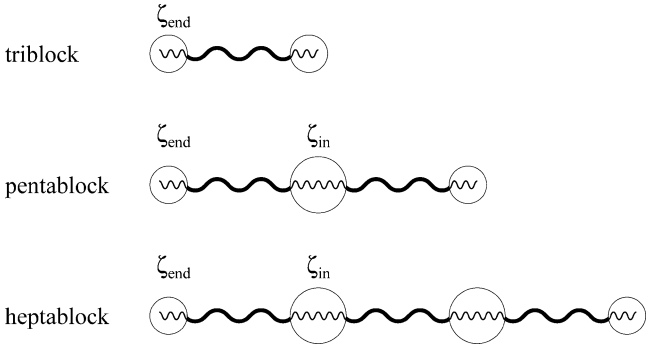

Figure 8. Schematic illustration of the triblock, pentablock, and heptablock chains having the effective friction coefficients ζ_{end} and ζ_{in} for the end and inner B blocks. These coefficients are determined by the B/S mixing barrier (required the thermal pullout of the B blocks from their domains). Note that the molecular weights of respective B and S blocks are (almost) identical for those chains (cf. Table 1).

gives an *effective* friction coefficient ζ_{end}, while the inner B block of the pentablock/heptablock chain gives ζ_{in}. Considering the difference of M_B of the end and inner B blocks, we may model these coefficients as

$$\zeta_{end} = K \exp(\Delta G_{15K}/k_B T) \tag{1a}$$

$$\zeta_{in} = K \exp(2\Delta G_{15K}/k_B T) \quad (>\zeta_{end}) \tag{1b}$$

Here, K is a proportionality constant, k_BT represents the thermal energy, and ΔG_{15K} denotes the barrier (free energy increment) for mixing the end B block of $M_B \cong 15 \times 10^3$ into the S/DBP matrix phase. The thermodynamic penalty for the B block in the matrix phase, determined by the S block molecular weight and concentration therein, should be very similar for all copolymers having almost identical M_S (cf. Table 1). Thus, we may consider ΔG_{15K} to be the same for the end B blocks of all copolymers. Similarly, the mixing barrier for the inner B block is the same for all copolymers. For the inner B blocks having $M_B \cong 30 \times 10^3$, the barrier should be twice of the barrier for the end B block, as specified in eq 1b. (The inner B block is less easily mixed in the matrix phase to give a larger ζ compared to the end B block.)

Now, we consider the equilibrium motion of the multiblock copolymer chain. We first need to examine whether the chain motion is affected by the entanglement. The motion of individual S blocks would be hardly affected by the (trapped) entanglement, as discussed earlier. However, the large-scale motion of the pentablock and heptablock chains involves several S blocks and could be affected by the entanglement.

When the copolymer chain exhibits the large-scale motion, the B block pulled out from its domain would have a collapsed conformation, and thus the entanglement between the copolymer chains should occur through their S blocks. In addition, the B blocks are minor components in the copolymers. For these reasons, the entanglement molecular weight for individual S blocks explained earlier, $M_e \cong 130 \times 10^3$, may be utilized as M_e for the copolymer chains. The total molecular weight of the S block(s) in the triblock chain, $M_{tot-S} \cong 160 \times 10^3$, is not sufficiently larger than M_e ($M_{tot-S} \cong 1.2M_e$), and thus motion of this chain should be free from the entanglement effect. This effect begins to emerge for the pentablock chain having $M_{tot-S} \cong 2.4M_e$ and becomes stronger for the pentablock chain having $M_{tot-S} \cong 3.6M_e$. Thus, we may assume the Rouse motion for the triblock chain, the reptation motion with contour length fluctuation (CLF) for the heptablock chain, and the crossover between of these types of motion for the pentablock chain. In

all cases, the large-scale motion of the copolymer chain is retarded by the B/S mixing on the pullout of the B block. This motion is conceptually similar to the sticky Rouse/reptation motion analyzed by Semenov and Rubinstein.[41−43]

From the above arguments, the characteristic time of the large-scale motion of the copolymer chains can be expressed in terms of the effective friction coefficients (eq 1), the radius of gyration R_g ($\sim M_{tot-S}^{1/2}$ for the copolymer chain with each B block in the collapsed state), and the equilibrium contour length L ($\sim M_{tot-S}$) as

$$\tau_{tri} = K'\{2\zeta_{end}\}R_{g,tri}^{\ 2} \qquad \text{for triblock chain} \tag{2}$$

$$\tau_{penta} = K'\{2\zeta_{end} + \zeta_{in}\}R_{g,penta}^{\ 2}$$

$$= K''\{2\zeta_{end} + \zeta_{in}\}L_{penta}^{\ 2.5} \qquad \text{for pentablock chain} \tag{3}$$

$$\tau_{hepta} = K''\{2\zeta_{end} + 2\zeta_{in}\}L_{hepta}^{\ 2.5} \qquad \text{for heptablock chain} \tag{4}$$

Here, K' and K'' are the proportionality constants. For the triblock and heptablock chains, the Rouse and reptation-CLF times are given by eqs 2 and 4, respectively. For the pentablock chain at the Rouse−reptation crossover, τ_{penta} is expressed in a dual form for these mechanisms (eq 3). Note in eqs 2−4 that the effective friction for the large-scale motion of the copolymer chain is not necessarily proportional to the chain molecular weight (because of the difference of the mixing barriers for the end and inner B blocks). Except this point, eqs 2−4 coincide with the standard expression for the Rouse/reptation times.[41−44]

For the multiblock solutions just above the microphase separation concentration (where the fluid−solid transition occurs), the mixing barrier ΔG_{15K} would be close to k_BT. Then, from eqs 2 and 3 with $\Delta G_{15K} = k_BT$, the τ_{penta}/τ_{tri} ratio is estimated to be

$$\frac{\tau_{penta}}{\tau_{tri}} = \frac{2\zeta_{end} + \zeta_{in}}{\zeta_{end}} \cong 4.7 \tag{5}$$

This ratio agrees well with the ratio of the elasticity recovery times observed for the triblock and pentablock chains, t_r^{∞}(penta)/t_r^{∞}(tri) ≅ 5. Furthermore, for $\Delta G_{15K} = k_BT$, eqs 3 and 4 give

$$\frac{\tau_{hepta}}{\tau_{penta}} = \frac{2\zeta_{end} + 2\zeta_{in}}{2\zeta_{end} + \zeta_{in}}\left(\frac{3}{2}\right)^{2.5} \cong 4.3 \tag{6}$$

This τ_{penta}/τ_{tri} ratio is again close to the observed ratio, t_r^{∞}(hepta)/t_r^{∞}(penta) ≅ 5. These results suggest that the elasticity recovery process (bridge re-formation process) is described by the Rouse/reptation dynamics retarded by the B/S mixing barrier.

3.5. Comment for Simultaneous Pullout of Many B Blocks. In relation to our simple model explained above, a comment needs to be added for the diffusion behavior observed for 2-vinylpyridine (P)−S−P triblock copolymers forming spherical P domains:[45,46] The diffusion of these copolymers occurs through two mechanisms: the "walking" mechanism, for which one P block is thermally pulled out from its domain and transferred to the other domain, and the "double activation" mechanism, for which two P blocks are pulled out simultaneously and the whole chain migrates. For high-M copolymers, the M dependence of the diffusion coefficient data strongly suggests that the walking mechanism governs the actual diffusion because the double activation mechanism is associated with a larger penalty of P/S mixing.

For our multiblock copolymers, the simultaneous pullout of many B blocks gives the effective friction coefficient ζ much larger than those given by eq 1: For example, if the two inner B blocks of the heptablock copolymer are simultaneously pulled out, ζ is given by $K \exp(4\Delta G_{15K}/k_BT)$. Our model is based on eq 1 and thus assumes no simultaneous pullout. In this sense, the molecular picture underlying this model is similar to the picture for the diffusion of the PSP copolymers.

4. Concluding Remarks

We have examined the rheology and structure for DBP solutions of a series of symmetrical multiblock copolymers, BSB triblock, BSBSB pentablock, and BSBSBSB heptablock copolymers having the same block molecular weights/composition. In a well-equilibrated state at 25 °C, these solutions formed a bcc lattice of the spherical B domains bridged by the S blocks (lattice-type network) to exhibit the elastic behavior against under small strains.

This lattice-type network was disrupted under steady shear to lose its elasticity, and the heaviest disruption occurred at an intermediate shear rate close to the B/S concentration fluctuation frequency. The elasticity was recovered after cessation of the preshear, and the time t_r^{∞} required for the full recovery was insensitive to the magnitude of the lattice disruption. This behavior suggested that the bridge-type S blocks are converted to the loops under the preshear and the re-formation of the bridges that stitch the flow plane (made by the preshear) is the rate-determining step for the elasticity recovery. The bridge re-formation is associated with the transient B/S mixing and thus gives $\dot{\gamma}_{pre}$-insensitive t_r^{∞}. In this sense, the triblock, pentablock, and heptablock copolymers exhibited similar behavior.

However, a quantitative difference was also noted for these copolymers. The elasticity recovery time t_r^{∞} increased with increasing copolymer molecular weight, and the ratio of t_r^{∞} of the triblock, pentablock, and heptablock copolymers was close to 1:5:25. This ratio can be explained by a simple model assuming the Rouse/reptation motion of the copolymer chains retarded by the B/S mixing on the bridge re-formation.

Acknowledgment. This work was supported by the Ministry of Education, Culture, and Sports, Science, and Technology, Japan (Grant No. 17350108).

Appendix. GPC Characterization of Copolymer Samples

The molecular weight of the first B block shown in Scheme 1, $M_{B1} = 15.5 \times 10^3$, was determined from the elution volume calibration and LALS measurement utilizing the monodisperse polybutadienes[34] as the reference. The weight fraction of the S block w_S in the BS diblock sample was determined from the RI and UV signal intensities of the sample, I_{RI} and I_{UV}, on the basis of the relationships valid at low SI concentration C

$$I_{RI} = K_{RI}\{\nu_S w_S + \nu_B(1 - w_S)\}C \tag{A1}$$

$$I_{UV} = K_{UV}\{\epsilon_S w_S + \epsilon_B(1 - w_S)\}C \tag{A2}$$

where ν_X and ϵ_X are the refractive index and UV adsorption increments per unit mass of the X block (X = S and B), respectively, and K_{RI} and K_{UV} are the instrument constants of the RI and UV monitors. ($\epsilon_B \cong 0$ at the UV wavelength of 254 nm utilized in our experiment.) The factors $\nu_X K_{RI}$ and $\epsilon_X K_{UV}$ were determined for solutions of standard polybutadienes and

polystyrenes of known concentrations. Thus, w_S was determined from the values of these factors and the measured I_{RI} and I_{UV} of the SI sample as

$$w_S = \frac{I_{UV}K_{RI}\nu_B - I_{RI}K_{UV}\epsilon_B}{I_{RI}K_{UV}(\epsilon_S - \epsilon_B) - I_{UV}K_{RI}(\nu_S - \nu_B)} \quad \text{(A3)}$$

The S block molecular weight (M_{S1} shown in Scheme 1) was determined from the w_S value and M_{B1} of the first B block as $M_{S1} = w_S M_{B1}/(1 - w_S)$.

For the precursor recovered after each step of the polymerization, the characterization was similarly made by utilizing an ex-precursor in the prior step. For example, for BSB^- (precursor for the pentablock sample), the ex-precursor was $BS1^-$ and a B block was copolymerized to $BS1^-$ (see Scheme 1). For BSB^-, an equation corresponding to eq A3 is written as

$$w_B^* = \frac{I_{UV}^{BSB}K_{RI}\nu_{ex} - I_{RI}^{BSB}K_{UV}\epsilon_{ex}}{I_{RI}^{BSB}K_{UV}(\epsilon_B - \epsilon_{ex}) - I_{UV}^{BSB}K_{RI}(\nu_B - \nu_{ex})} \quad \text{(A4)}$$

where w_B^* is the weight fraction of the copolymerized B block (third block in BSB), and ν_{ex} and ϵ_{ex} are the refractive index and UV adsorption increments per unit mass of the ex-precursor BS1. Thus, w_B^* is evaluated from the factors $\nu_{ex}K_{RI}$ and $\epsilon_{ex}K_{UV}$ determined for BS1 and the RI and UV signal intensities I_{RI}^{BSB} and I_{UV}^{BSB} measured for BSB. Since the BS1 molecular weight M_{SB1} was known (through the characterization on the basis of eqs A1−A3), the molecular weight M_{B2} of the third B block in BSB was determined from the w_B^* value as $M_{B2} = w_B^* M_{SB1}/(1 - w_B^*)$.

All precursors were characterized sequentially with the above method. The RI/UV signal ratios measured for the BSB triblock, BSBSB pentablock, and BSBSBSB heptablock samples coincided with the ratios for respective precursors, but the retention times for the samples were shorter than those of the precursors by a factor that corresponded to doubling the molecular weight. Thus, the block molecular weights of the triblock, pentablock, and heptablock samples were calculated from those of the precursors. The star block sample exhibited the RI/UV signal intensity ratio identical to that for its precursor BS and had the retention time expected for a four-arm star, and the block molecular weights of this sample was calculated from those of the precursor BS. The results are summarized in Table 1.

References and Notes

(1) Watanabe, H. Rheology of Multiphase Polymeric Systems. In Araki, T., Qui, T. C., Shibayama, M., Eds.; *Structure and Properties of Multiphase Polymeric Materials*; Marcel Dekker: New York, 1998; Chapter 9.
(2) Chung, C. I.; Gale, J. C. *J. Polym. Sci., Phys. Ed.* **1976**, *14*, 1149.
(3) Gouinlock, E. V.; Porter, R. S. *Polym. Eng. Sci.* **1977**, *17*, 535.
(4) Pico, E. R.; Williams, M. C. *Polym. Eng. Sci.* **1977**, *17*, 573.
(5) Morrison, F. A.; Winter, H. *Macromolecules* **1989**, *22*, 3533.
(6) Morrison, F. A.; Winter, H.; Gronski, W.; Barnes, J. D. *Macromolecules* **1990**, *23*, 4200.
(7) Watanabe, H.; Kuwahara, S.; Kotaka, T. *J. Rheol.* **1984**, *28*, 393.
(8) Sato, T.; Watanabe, H.; Osaki, K. *Macromolecules* **1996**, *29*, 6231.
(9) Watanabe, H.; Sato, T.; Osaki, K.; Yao, M. L.; Yamagishi, A. *Macromolecules* **1997**, *30*, 5877.
(10) Watanabe, H.; Sato, T.; Osaki, K. *Macromolecules* **2000**, *33*, 2545.
(11) Hamley, I. W.; Fairclough, J. P. A.; Ryan, A. J.; Ryu, C. Y.; Lodge, T. P.; Gleeson, A. J.; Pedersen, J. S. *Macromolecules* **1998**, *31*, 1188.
(12) Spontak, R. J.; Wilder, E. A.; Smith, S. D. *Langmuir* **2001**, *17*, 2294.
(13) Laurer, J. H.; Khan, S. A.; Spontak, R. J.; Satkowski, M. M.; Grothaus, J. T.; Smith, S. D.; Lin, J. S. *Langmuir* **1999**, *15*, 7947.
(14) Watanabe, H.; Kotaka, T.; Hashimoto, T.; Shibayama, M.; Kawai, H. *J. Rheol.* **1982**, *26*, 153.
(15) Watanabe, H.; Kotaka, T. *J. Rheol.* **1983**, *27*, 223.
(16) Watanabe, H. *Acta Polym.* **1997**, *48*, 215.
(17) Watanabe, H.; Kanaya, T.; Takahashi, Y. *Macromolecules* **2001**, *34*, 662.
(18) McConnell, G. A.; Lin, M. Y.; Gast, A. P. *Macromolecules* **1995**, *28*, 6754.
(19) Watanabe, H.; Matsumiya, Y.; Kanaya, T.; Takahashi, T. *Macromolecules* **2001**, *34*, 6742.
(20) Lodge, T. P.; Xu, X.; Ryu, C. Y.; Hamley, I. W.; Fairclough, J. P. A.; Ryan, A. J.; Pedersen, J. S. *Macromolecules* **1996**, *29*, 5955.
(21) Hanley, K. J.; Lodge, T. P.; Huang, C. I. *Macromolecules* **2000**, *33*, 5918.
(22) Tan, H.; Watanabe, H.; Matsumiya, Y.; Kanaya, T.; Takahashi, Y. *Macromolecules* **2003**, *36*, 2886.
(23) Takano, A.; Kamaya, I.; Takahashi, Y.; Matsushita, Y. *Macromolecules* **2005**, *38*, 9718.
(24) Takahashi, Y.; Song, Y. H.; Nemoto, N.; Takano, A.; Akazawa, Y.; Matsushita, Y. *Macromolecules* **2005**, *38*, 9724.
(25) Hashimoto, T.; Shibayama, M.; Kawai, H. *Macromolecules* **1980**, *13*, 1237.
(26) Watanabe, H. *Macromolecules* **1995**, *28*, 5006.
(27) Matsen, M. W. *J. Chem. Phys.* **1995**, *102*, 3884.
(28) Matsen, M. W.; Schick, M. *Macromolecules* **1994**, *27*, 187.
(29) Morton, M.; Fetters, L. J. *Rubber Chem. Technol.* **1975**, *48*, 359.
(30) Morton, M. *Anionic Polymerization: Principles and Practice*; Academic Press: New York, 1983.
(31) Fujimoto, T.; Nagasawa, M. *Advanced Techniques for Polymer Synthesis*; Kagaku-Dojin: Kyoto, 1972.
(32) Gervasi, J. A.; Gosnell, A. B. *J. Polym. Sci., Polym. Chem. Ed.* **1966**, *4*, 1391.
(33) Watanabe, H.; Yoshida, H.; Kotaka, T. *Macromolecules* **1988**, *21*, 2175.
(34) Watanabe, H.; Urakawa, O.; Kotaka, T. *Macromolecules* **1994**, *27*, 3525.
(35) Takahashi, Y.; Noda, M.; Naruse, M.; Kanaya, T.; Watanabe, H.; Kato, T.; Imai, M.; Matsushita, Y. *Nihon Reoroji Gakkaishi* (*J. Soc. Rheol. Jpn.*) **2000**, *28*, 187.
(36) Mandare, P.; Horst, R.; Winter, H. H. *Rheol. Acta* **2005**, *45*, 33.
(37) Ferry, J. D. *Viscoelastic Properties of Polymers*, 3rd ed.; Wiley: New York, 1980.
(38) Watanabe, H.; Kotaka, T. *Macromolecules* **1986**, *19*, 2520.
(39) The sample solutions were subjected to the heat treatment at 70 °C prior to the measurement. However, their G' data at 70 °C suggested that the multiblock solutions remained phase-separated to some extent at 70 °C. Thus, the (trapped) entanglement in these solutions should have been mainly formed during the cosolvent evaporation in the solution preparation procedure.
(40) In principle, the elasticity recovery for the BS diblock solution proceeds through competition of the motion of the B domains and the thermal migration of BS chains from one domain to the others. For the BS chain in the nonentangled state, a time τ_{di} required for the migration is estimated from an equation similar to eq 2: $\tau_{di} = K'\zeta_{end}R_{g,di}^2 = \tau_{tri}/4$, where K' and ζ_{end} are the proportionality constant and effective friction coefficient explained for eqs 1 and 2, $R_{g,di}$ is the radius of gyration of the BS chain, and τ_{tri} is the migration time for the triblock chain (cf. eq 2). The τ_{di}/τ_{tri} ratio (=1/4) is much larger than the ratio observed in Figure 7, suggesting that the elasticity recovery in the BS diblock solution is governed by the motion of the B domains.
(41) Rubinstein, M.; Semenov, A. N. *Macromolecules* **1998**, *31*, 1386.
(42) Rubinstein, M.; Semenov, A. N. *Macromolecules* **2001**, *34*, 1058.
(43) Semenov, A. N.; Rubinstein, M. *Macromolecules* **2002**, *35*, 4821.
(44) Doi, M.; Edwrads, S. F. *The Theory of Polymer Dynamics*; Oxford: Clarendon, 1986.
(45) Yokoyama, H.; Kramer, E. *Macromolecules* **2000**, *33*, 954.
(46) Yokoyama, H. *Mater. Sci. Eng. R* **2006**, *53*, 199.

MA070306R